Perfectly Matched Layer Behavior in Negative Refractive Index Materials

Steven A. Cummer, *Senior Member, IEEE*

Abstract—The perfectly matched layer (PML) absorbing boundary condition is shown to be analytically unstable for a material with a bandwidth of negative refractive index. Physically, this is a consequence of the reversed phase and group velocities in such a medium. The instability is inherent in the PML and is not implementation-specific. We derive a modified PML (NIMPML) that is analytically stable in a negative index material (NIM), and we demonstrate its numerical stability in a specific NIMPML implementation.

Index Terms—Absorbing boundary condition, negative index material, perfectly matched layer.

I. INTRODUCTION

NEGATIVE refractive index materials (NIMs) have many unusual and potentially useful properties [1]. Moreover, they are constructable at microwave frequencies using simple resonant metallic inclusions in a uniform dielectric [2], [3]. Finite difference simulations of wave propagation in these materials have proven useful in investigating some of these unusual properties [4]–[6], and should prove similarly useful in realistic simulations of potential applications.

Simulations of NIM properties and applications may require absorbing boundary conditions (ABCs) to truncate the computational domain at the edges of a negative index material. These materials are necessarily highly dispersive [7] and thus not every ABC is easily adaptable to solve unbounded NIM simulations. The perfectly matched layer is a versatile ABC that has been adapted to linear dispersive materials in a variety of slightly different formulations [8]–[11] and can, in theory, be adapted to NIM simulations. However, we show analytically that standard versions of the perfectly matched layer (PML) are inherently unstable in materials with a bandwidth of frequencies with negative refractive index. This conclusion is confirmed by simple simulations.

We also present and demonstrate a modified PML that is analytically stable for unbounded NIMs. We call this the NIMPML, and it is only slightly more complicated to implement than the regular PML. The NIMPML requires coupling a finite difference approximation of a second-order ordinary differential equation to the discretized Maxwell equations, and we show that there is at least one implementation that is numerically stable when coupled to the Maxwell equations.

II. PML INSTABILITY IN NEGATIVE INDEX MATERIALS

We use the $\exp(j\omega t)$ time convention. Gedney [8], straightforwardly extending the results of Sacks *et al.* [12], showed that the permittivity and permeability of an absorbing PML in an isotropic linear dispersive medium can be written as $\epsilon = \epsilon_0\epsilon_r(\omega)\bar{\bar{s}}$ and $\mu = \mu_0\mu_r(\omega)\bar{\bar{s}}$ with

$$\bar{\bar{s}} = \begin{bmatrix} 1 + \frac{\sigma}{j\omega} & 0 & 0 \\ 0 & 1 + \frac{\sigma}{j\omega} & 0 \\ 0 & 0 & \left(1 + \frac{\sigma}{j\omega}\right)^{-1} \end{bmatrix} \quad (1)$$

where $\mu_r(\omega)$ and $\epsilon_r(\omega)$ are the frequency-dependent relative permeability and permittivity, respectively, of the dispersive medium. The parameter σ is the standard PML loss parameter [13] that controls the wave attenuation rate in the PML. We consider two-dimensional (2-D) fields ($\partial/\partial y = 0$) of either polarization in a z-absorbing PML to demonstrate the instability. Assuming a plane wave solution with fields varying as $\exp(-j(k_x x + k_z z))$, it is straightforward from (1) to show that the fields in the PML obey the dispersion relation

$$\frac{k_z^2}{\left(1 + \frac{\sigma}{j\omega}\right)^2} + k_x^2 = \frac{\omega^2}{c^2}\mu_r\epsilon_r. \quad (2)$$

Letting $\bar{k}_z = k_z/(1 + \sigma/j\omega)$, the fields become spatially dependent on the factor

$$\exp(-j\bar{k}_z z)\exp(-jk_x x)\exp\left(-\frac{\bar{k}_z\sigma z}{\omega}\right) \quad (3)$$

where $\bar{k}_z$ and k_x satisfy the non-PML dispersion relation $\bar{k}_z^2 + k_x^2 = (\omega/c)^2\mu_r\epsilon_r$.

Equation (3) shows that the PML fields decay in the direction of the z component of the wavenumber $\bar{k}_z$. In other words, the fields decay in the direction of the phase velocity of the wave. In an ordinary positive index medium, the directions of power flow and phase velocity are commonly parallel and at least not anti-parallel. Thus, the field energy leaves the computational domain in the same direction as the phase velocity, and the field amplitude consequently decays as it should in an ABC.

In an isotropic NIM, phase velocity and power flow are antiparallel, and energy leaves the computational domain in waves with a phase velocity pointing back into the domain. According to (3), this energy must also decay in the direction of its phase velocity. However, in this case, this implies exponential field *growth* as the energy leaves the domain. Consequently, the standard PML is unstable in a negative index material. This result applies in one, two, or three dimensions, and also applies to any

medium in which the components of energy flow and phase velocity in the direction of PML absorption are antiparallel. In the final section, we demonstrate this instability numerically.

III. STABLE PML FOR NEGATIVE INDEX MATERIALS

The factor $1 + \sigma/j\omega$ in (1), which we from here on refer to as s following the notation in the stretched coordinate derivation of the PML [14], can be replaced with any other function and it will still act as a perfectly matched layer [12] (though it may not be absorbing). If s is a rational function of $j\omega$, then its time domain equivalent is a linear ordinary differential equation that can be coupled to the Maxwell equations in a finite difference approximation. For a stable NIMPML, we thus require an s that is rational in $j\omega$ and, most importantly, changes sign in the frequency band where the material has a negative index. For a material where $\epsilon_r = \mu_r = 1 - \omega_p^2/\omega^2$, the refractive index $n < 0$ for $\omega < \omega_p$ (this material was considered by [4]) and a good choice for s is

$$s = 1 + \frac{\sigma}{j\omega \left(1 - \frac{\omega_p^2}{\omega^2}\right)}. \tag{4}$$

It is straightforward to show through (2) and (3) that this modification, when applied to this medium, results in a PML where the fields decay as $\exp(-\sigma z/c)$ independent of frequency and refractive index. In general, the choice

$$s = 1 + \frac{\sigma}{j\omega\sqrt{\mu_r\epsilon_r}} \tag{5}$$

ensures that the PML decay direction is not phase velocity dependent. The sign of the square root should correspond to the fields that carry power out of the computational domain. A PML for a NIM realization with resonant material responses, namely $\epsilon_r = \mu_r = 1 + \omega_p^2/(\omega_0^2 - \omega^2)$, can be derived in the same way.

A limitation of the NIMPML as outlined before is that in a NIM in which $\epsilon_r \neq \mu_r$ (for example, the electric cutoff and magnetic resonance achieved through a wire/split ring resonator medium [2]), $\sqrt{\mu_r\epsilon_r}$ is not a rational function of $j\omega$. Equation (5) would not be equivalent to a time domain ordinary differential equation and could not be directly coupled to the Maxwell equations as we describe below. This limitation does not inhibit use of the NIMPML in simulations of basic NIM properties and behavior. Many interesting NIM phenomena and applications depend only on the existence of a negative index and are not strongly dependent on the specific functional form of the permittivity and permeability. Either the two cutoff or two resonance form can thus be used in many cases to simulate realistically the behavior of more general NIMs. We also suggest without further investigation that it may be possible to stabilize a PML in such a NIM by using an s with electric and magnetic resonances that give a negative index in the same frequency band (though with a different functional form) as the non-PML medium.

IV. NIMPML IMPLEMENTATION

With the function s (which can be thought of as either a uniaxial permittivity/permeability element or a complex coordinate stretch) defined, the NIMPML can be implemented in many different ways. However, because (4) is equivalent to a second order time domain ordinary differential equation, a split field
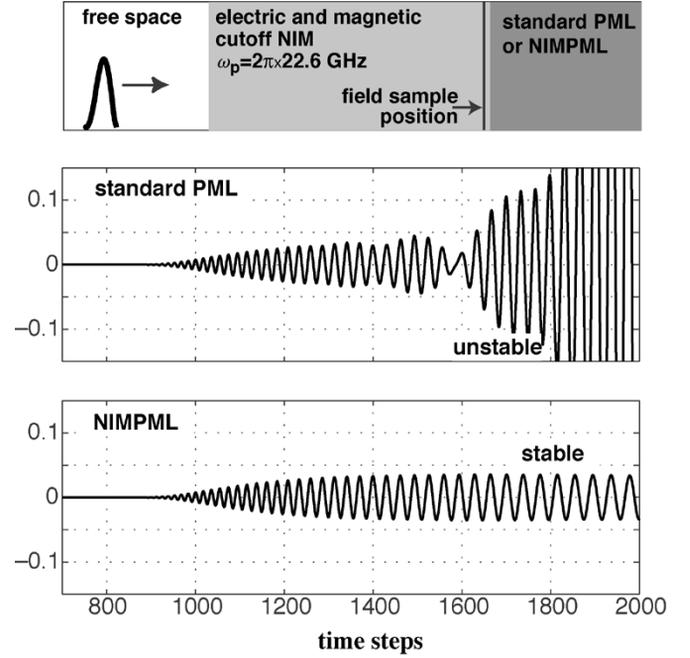

Fig. 1. (Top) Schematic of the numerical simulation. A broadband pulse is incident on a NIM halfspace truncated with a standard PML or NIMPML. (Middle) Time domain field recorded adjacent to the standard PML is clearly unstable. (Bottom) Time domain field recorded adjacent to the NIMPML is stable.

implementation would require multiple time derivatives of field curls and thus would be rather complicated. We derive a straightforward implementation below and numerically demonstrate its stability.

Following [11], the fields in the NIMPML can be written as the Maxwell equations containing modified fields $\bar{E}$ and $\bar{H}$ where $\bar{F} = F/s$ (F is either E or H). Note that $\bar{F}$ here is called $\tilde{F}$ in [11]; we have changed the nomenclature to avoid confusion with a different variable change denoted by $\tilde{\cdot}$ in some PML literature.

From (4), and converting to the time domain

$$\left(\frac{d^2}{dt^2} + \sigma\frac{d}{dt} + \omega_p^2\right)\bar{F} = \left(\frac{d^2}{dt^2} + \omega_p^2\right)F. \tag{6}$$

This ordinary differential equation for E and H can be coupled to the Maxwell equations containing instances of the fields $\bar{E}$ and $\bar{H}$. In a leapfrog finite difference approximation, we thus have the following iterative steps: E from $\bar{H}$ from the Maxwell equations, $\bar{E}$ from E from (6), H from $\bar{E}$ from the Maxwell equations, and $\bar{H}$ from H from (6).

We implement a centered second-order finite difference approximation of (6) as

$$\bar{F}^{n+1}\left(1 + \frac{\sigma\Delta t}{2} + \frac{\omega_p^2\Delta t^2}{4}\right)$$
$$= \bar{F}^n\left(2 - \frac{\omega_p^2\Delta t^2}{2}\right) + \bar{F}^{n-1}\left(-1 + \frac{\sigma\Delta t}{2} - \frac{\omega_p^2\Delta t^2}{4}\right)$$
$$+ F^{n+1}\left(1 + \frac{\omega_p^2\Delta t^2}{4}\right) + F^n\left(\frac{\omega_p^2\Delta t^2}{2} - 2\right)$$
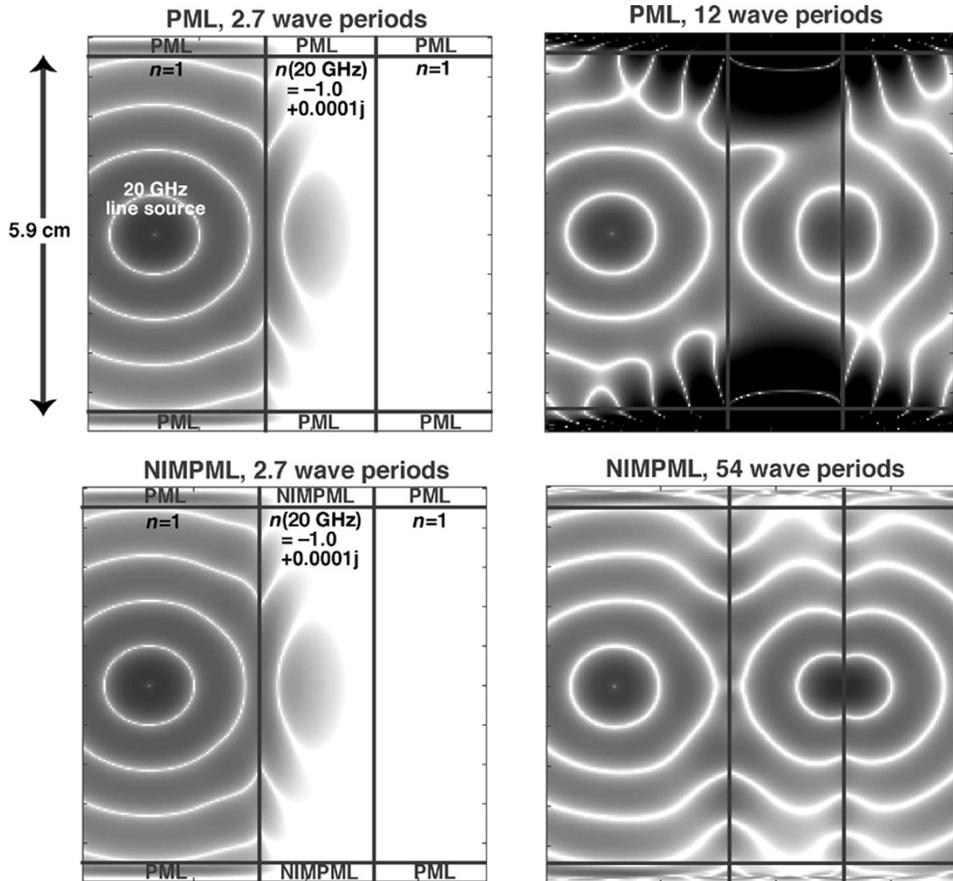$$+ F^{n-1}\left(1 + \frac{\omega_p^2\Delta t^2}{4}\right) \tag{7}$$

Fig. 2. Fields from time harmonic line source simulation with NIM slab. (Top) Standard PML is used to terminate the NIM slab. After 12 source periods a strong instability is evident in the PML edges of the NIM slab. (Bottom) Using the NIMPML, the same simulation is stable for at least 54 source periods and is able to produce the desired steady state solution.

and numerically demonstrate later that it is sufficiently stable at the Courant condition $c\Delta t/\Delta x \leq 1/\sqrt{(\dim)}$ (dim is the dimensionality of the problem) to give good results. Note that this form approximates the F term in (6) as $(F^{n+1}+2F^n+F^{n-1})/4$ rather than F^n. We find the latter approximation unstable when linked to the discrete Maxwell equations despite being centered, second order accurate, and stable as an ordinary differential equation approximation.

We have considered only lossless NIMs previously. To simulate some NIM phenomena, for instance subwavelength focusing, loss must be included to ensure that a steady state is reached [5], [15]. A simulation of physically realizable NIMs will normally include at least some loss. Including loss is straightforward with the lossy cutoff and resonant forms ϵ_r, $\mu_r = 1-\omega_p^2/(\omega^2 - j\omega\nu)$ and ϵ_r, $\mu_r = 1+\omega_p^2/(\omega_0^2+j\omega\nu-\omega^2)$, respectively, where ν is a loss parameter. These lossy forms can be used to derive slightly more complicated versions of (6) so that (5) is satisfied. However, in practice we find that the lossless (7) can be used with a lossy NIM without significant impact on performance.

V. SIMULATIONS

To demonstrate both the instability of the standard PML and stability of the NIMPML, we implemented a one-dimensional (1-D) leapfrog finite difference approximation of a material with a magnetic and electric plasma response: $\mu_r = \epsilon_r = 1-\omega_p^2/\omega^2$, with $\omega_p = 2\pi \times 22.6$ GHz. A narrow, broadband, plane wave pulse (0–30 GHz) is incident from free space on a half space of this negative index material. The NIM is truncated 0.26 m from the material interface with a standard PML and the NIMPML, each 50-cells long with a 5/2-power polynomial increase of σ with distance and with $\sigma_{\max} = 0.2/\Delta t$. Fig. 1 shows the electric field waveform recorded adjacent to the PML in each case. The signal after 0.26 m propagation through this very dispersive medium is spread broadly in time. Most importantly, the standard PML simulation is unstable, while the NIMPML simulation is stable enough to compute a solution for at least 4000 time steps. Moreover (not shown but easily seen in the simulations), the standard PML is stable until the energy contained in the negative index band (which travels at a group velocity significantly less than c) arrives at the PML. This explains the delayed instability onset in Fig. 1 and confirms our analysis that showed the instability of the standard PML is only in the negative index frequency band.

For lossless and very-low loss NIMs in the above simulation, we find a slowly developing, narrow bandwidth instability in the NIMPML at the $n = 0$ frequency (in this case, 22.6 GHz) that can eventually swamp the desired solution after long times (in this case, about 10^4 time steps). Unusual behavior at $n = 0$ is not especially surprising in light of the division by $n = \sqrt{\mu_r\epsilon_r}$ in (5). We find empirically that this instability can

be reduced in practice by adding some loss to the Maxwell equations in the NIMPML. This creates a slight mismatch between the NIMPML and the NIM, but in practice we find that reflections are still very small and the 1-D simulation can be made stable until at least 10^5 timesteps (the simulation was not run any longer). It is also possible that adding some loss to the NIMPML through (6), as discussed in the above section, may also eliminate this slowly developing $n = 0$ instability.

To demonstrate the performance and value of the NIMPML in a more interesting, two-dimensional problem, we compare the NIMPML and the standard PML in Fig. 2. A harmonic (20-GHz) line current source in free space is next to a slab of slightly lossy electric and magnetic cutoff NIM with $n(20 \text{ GHz}) = -1.0 + 0.0001j$. In this configuration, the source radiation will be focused on the far edge of the NIM slab [16]. To simulate a transversely infinite NIM slab, we used a standard PML and the NIMPML derived above as absorbing boundary conditions, each ten cells long with a cubic polynomial increase of σ with distance and with $\sigma_{\max} = 3/\Delta t$.

In both simulations, the early time fields show identical initial focusing of the source radiation. After 12 source periods, the standard PML is unstable in the NIM and the solution is very nearly swamped. The NIMPML simulation, in constrast, exhibits no instability after 54 source periods and has essentially reached the desired steady state.

VI. CONCLUSION

Applying the standard perfectly matched layer to a dispersive negative refractive index material results in analytical instability in the negative index band due to the antiparallel phase velocity and power flow in such a medium. A modified PML is derived that corrects for this fact and results in a stable absorbing boundary condition that we call the NIMPML. The NIMPML can be implemented in any of the common PML forms and is only slightly more complicated than the standard PML. 1-D and 2-D simulations confirm both the instability of the standard PML and the stability of the NIMPML. The NIMPML thus enables finite difference simulations of unbounded negative index

materials so that the fundamental properties of NIMs, and their performance in applications, can be explored and quantified.

REFERENCES

[1] V. G. Veselago, "Electrodynamics of substances with simultaneously negative values of ϵ and μ," *Sov. Phys. Usp.*, vol. 10, p. 509, 1968.

[2] D. R. Smith, W. J. Padilla, D. C. Vier, S. C. Nemat-Nasser, and S. Schultz, "Composite medium with simultaneously negative permeability and permittivity," *Phys. Rev. Lett.*, vol. 84, pp. 4184–4187, May 2000.

[3] R. A. Shelby, D. R. Smith, and S. Schultz, "Experimental verification of a negative index of refraction," *Science*, vol. 292, no. 5514, pp. 77–79, Apr. 2001.

[4] R. W. Ziolkowski and E. Heyman, "Wave propagation in media having negative permittivity and permeability," *Phys. Rev. E*, vol. 64, no. 5, p. 056 625, Nov. 2001.

[5] S. A. Cummer, "Simulated causal subwavelength focusing by a negative refractive index slab," *Appl. Phys. Lett.*, vol. 82, no. 10, pp. 1503–1505, Mar. 2003.

[6] ——, "Dynamics of causal beam refraction in negative refractive index materials," *Appl. Phys. Lett.*, vol. 82, no. 13, pp. 2008–2010, Mar. 2003.

[7] D. R. Smith and N. Kroll, "Negative refractive index in left-handed metamaterials," *Phys. Rev. Lett.*, vol. 85, no. 14, pp. 2933–2936, Oct. 2000.

[8] S. D. Gedney, "An anisotropic PML absorbing media for the FDTD simulation of fields in lossy and dispersive media," *Electromagn.*, vol. 16, pp. 399–415, 1996.

[9] G. X. Fan and Q. H. Liu, "An FDTD algorithm with perfectly matched layers for general dispersive media," *IEEE Trans. Antennas Propagat.*, vol. 48, pp. 637–646, May 2000.

[10] J. A. Roden and S. D. Gedney, "Convolution PML (CPML): An efficient FDTD implementation of the CFS-PML for arbitrary media," *Microwave Opt. Technol. Lett.*, vol. 27, no. 5, pp. 334–339, 2000.

[11] S. A. Cummer, "A simple, nearly perfectly matched layer for general electromagnetic media," *IEEE Microwave Wireless Compon. Lett.*, vol. 13, pp. 128–130, Mar. 2003.

[12] Z. S. Sacks, D. M. Kingsland, R. Lee, and J. F. Lee, "A perfectly matched anisotropic absorber for use as an absorbing boundary condition," *IEEE Trans. Antennas Propagat.*, vol. 43, pp. 1460–1463, Dec. 1995.

[13] J.-P. Berenger, "A perfectly matched layer for the absorption of electromagnetic waves," *J. Comput. Phys.*, vol. 114, no. 2, pp. 185–200, 1994.

[14] W. C. Chew and W. H. Weedon, "A 3D perfectly matched medium from modified Maxwell's equations with stretched coordinates," *Microwave Opt. Technol. Lett.*, vol. 7, no. 13, pp. 599–604, Sept. 1994.

[15] G. Gómez-Santos, "Universal features of the time evolution of evanescent modes in a left-handed perfect lens," *Phys. Rev. Lett.*, vol. 90, Feb. 2003.

[16] J. B. Pendry, "Negative refraction makes a perfect lens," *Phys. Rev. Lett.*, vol. 85, no. 18, pp. 3966–3969, Oct. 2000.